International Conference on Applied Energy 2019
Aug 12-15, 2019, Västerås, Sweden
Paper ID: 0736

EXPERIMENTAL STUDY ON HEAT TRANSFER ENHANCEMENT DURING CONDENSATION USING MICROSTRUCTURED SURFACES

Haydee Martinez-Zavala*, Debajyoti Bhaduri, Agustin Valera-Medina, Samuel Bigot

School of Engineering, Cardiff University, Queen's Buildings, The Parade, Cardiff, CF24 3AA, United Kingdom

ABSTRACT

Microstructured surfaces have been found to be energy efficient and cost effective through enhancement of heat transfer, drag reduction and anti-fouling in areas such as thermal engineering, fluid mechanics, microelectronics and transportation. However, their use with the condensation phenomenon has yet to receive considerable attention. Therefore, based on a new approach to recover energy in humid environments, the influence of different geometries manufactured on stainless steel inserts via micro-wire electro discharge machining (μ-WEDM) on condensation was analysed. The experimental work was carried out in a chamber with a high percentage of relative humidity (% RH) comparing the geometries against an unstructured surface. The experimental results showed a differential temperature (ΔT), 26% higher than the unstructured surface. Thus, it is reasonable to believe that this experimental study could be used in the design of energy recovery systems to enhance condensation heat transfer.

Keywords: Microstructured Surfaces, Heat Transfer Enhancement, Condensation, Biomimetic Engineering, μ-WEDM.

NOMENCLATURE

Abbreviations	
μ-WEDM	Micro-wire electro discharge machining
RH	Relative humidity
DWC	Dropwise condensation
FWC	Filmwise condensation
Symbols	
$\dot{Q}$	Rate of heat transfer
ΔT	Differential temperature

1. INTRODUCTION

Reduction of greenhouse gases through the efficient use of energy can be achieved by imitating nature through biomimetic engineering. Microstructured surfaces are already being used in transport applications, aerospace and medical equipment, combustion systems and heat transfer processes for the reduction of energy consumption, vehicle stabilisation, surface self-cleaning, stabilisation of flashback in swirl burners, electronics cooling, heat exchangers, heat sinks, boiling and thermal control in nuclear power plants and so on. Nevertheless, their application with the condensation phenomenon has not received the same attention as in liquid cooling and boiling for phase change enhancement [1–7]. Due to its high heat transfer coefficient, vapour condensation has been widely utilised in chemical and environmental engineering processes, refrigeration and power generation sectors [8].

Extremely energetic meteorological phenomena with humid environments, such as storms, contain an enormous amount of energy [9]. Thus, the use of microstructured surfaces, that can improve condensation heat transfer between these phenomena and energy recovery systems, represents a new futuristic alternative energy source that could support the reduction of fossil fuels' consumptions.

Therefore, the objective of this experimental study is to provide some fundamental information, such as microstructure geometry, in order to develop a system capable of recovering all the energy in humid environments. Furthermore, the results can be used in other heat transfer applications and can also expand the applications for other high-value manufacturing and materials science sectors.

Selection and peer-review under responsibility of the scientific committee of the 11th Int. Conf. on Applied Energy (ICAE2019).

2. THEORY

Enhancement of condensation heat transfer can be achieved through the modification of physical and chemical properties of the surface [10]. Consequently, microstructured surfaces can help to ensure high heat transfer in locations with high humidity levels by transferring the energy from the large latent heat, associated with the phase change to the surface of the device, instead of passing it to the drier air. This phenomenon is based on the generation of micro-vortical motion encapsulated in solid valleys, which due to rotation, keeps a continuous exchange of energy while maintaining a single point-in-contact with the solid surface and thereby reduces drag and pressure losses [11]. Furthermore, research in this area has been successfully undertaken using specific surfaces to increase heat transfer and detachment of droplets whilst delaying surface flooding [2].

Surface condensation can take place through two mechanisms: Dropwise Condensation (DWC) and Filmwise Condensation (FWC). On unstructured surfaces, it depends on the nature of the fluid, the ambient conditions, the liquid-gas surface tension and surface energy; while on microstructured surfaces, their physical structure and the chemical heterogeneities also play a major role [2]. Numerical and experimental studies demonstrated heat transfer enhancement when grooved surfaces were used to decrease liquid film thickness [8]. Even though FWC offers an order of magnitude lower heat transfer coefficients than DWC due to the thickness of liquid film covering the solid surface, Orejon et al. [2] demonstrated a good heat transfer performance with simultaneous DWC/FWC by varying the microstructured surfaces design parameters.

Due to the complexity of the microstructured surfaces geometries and the condensation mechanisms that could be presented during the experimental phase, the following arguments were considered: (1) The vapour velocity is very low (0.15 m/s), therefore the interfacial shear between the liquid and the vapour is negligible [8]. (2) The rate of heat transfer ($\dot{Q}$) is directly proportional to the differential temperature (ΔT). (3) The inserts used for the experiments possess the same properties with a marginal difference in the total microstructured surface areas among them, and hence can be considered negligible. Thus, ΔT becomes the main parameter for this study.

Temperature (K)	Relative Humidity (%)	Pressure (bar)
301.57 ± 0.5%	96 ± 3%	1.02 ± 0.5%

Table 1. Experimental conditions in the chamber.

3. MATERIALS AND METHODS

Taking into account the application of the microstructured surfaces in the energy recovery from energetic meteorological phenomena in humid environments, the conditions for the experiments in Table 1 were chosen according to the statistical analysis and collection of data by The National Oceanic and Atmospheric Administration (NOAA) at temperatures above 26°C (299.15 K) where the %RH is between 75% and 100% at the inner core of large storms and between 63% and 96.5% at the periphery of the storm [12]. Each set of experiments was carried out for a period of 8 minutes to corroborate repeatability under stable conditions. Temperature and %RH measurements inside the chamber were recorded every 20 seconds whereas the inserts' surface temperatures were measured after every 10 seconds.

3.1 Inserts with microstructured surfaces

The stainless steel (grade 316L) inserts were manufactured via casting followed by machining. The height of the inserts was 25 mm of which the bottom 10 mm had a diameter of 28 mm while the top 15 mm had a diameter of 25 mm (Figure 1a). The top faces of the 25 mm diameter section were machined (roughness R_a = 0.2 μm) prior to the fabrication of the microstructures which were created via μ-WEDM. More details about the generation of the microstructures are presented in the study by Al-fahham et al. [13]. The selection of the geometries was based on the extensive research available on the properties of shark skin and lotus leaves [14–17]. However, a major factor for the selection was the limitations presented by the manufacturing technique. Hence, simpler geometries, such as scallop and diamond, were also chosen.

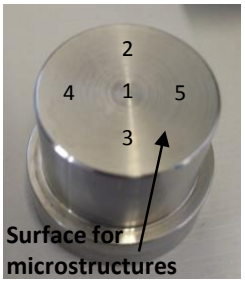

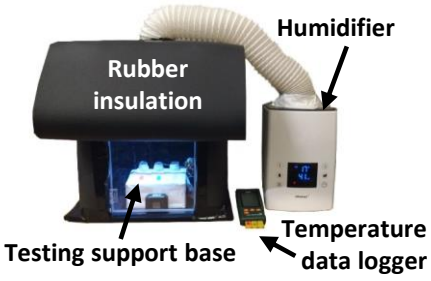

Figure 1a. A machined unstructured insert
Figure 1b. Experimental apparatus for the condensation heat transfer experiments.

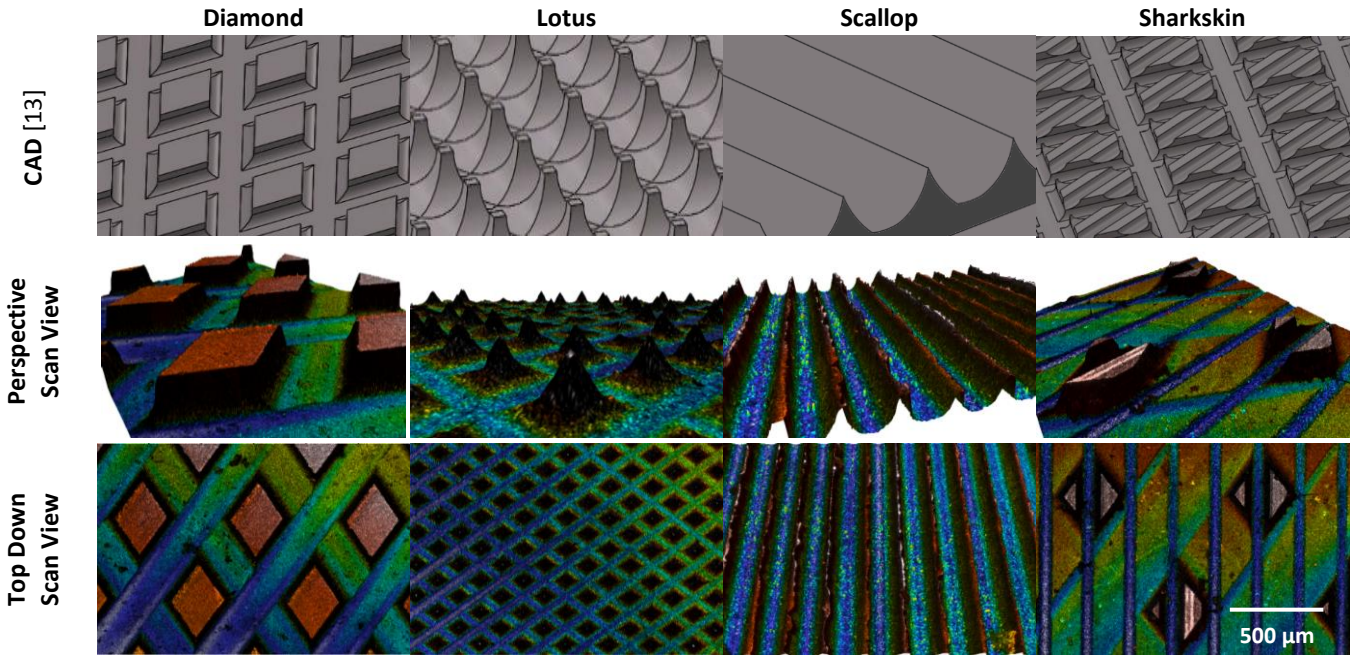

Figure 2. CAD designs and scanned geometries of the microstructured surfaces.

3.2 Characterisation of the microstructured surfaces

The computer aided drawing (CAD) for each of the microstructure geometries is shown in Figure 2. After creating the insert, an optical 3D scanner 'Sensofar Smart' was used for scanning of each geometry. The perspective and the top down scaled views of the scans are shown in Figure 2. For the characterisation, five areas of dimension 1.7 mm × 1.4 mm were scanned on the structured 25 mm inserts' top faces, the approximate locations of which are shown on an equivalent unstructured surface in Figure 1a. Each of the scanned areas was divided into three sections from where five measurement points were chosen. At each point, three different groove characteristics were measured: widths and depths of the grooves, and widths of the riblets. Thus, a total of 75 measurements were taken on each insert. The averages of the measured data are presented in Table 2.

Geometry	Width of grooves (µm)	Depth of grooves (µm)	Width of riblets (µm)
Diamond	278.39	121.71	251.70
Lotus	126.21	54.79	16.66
Scallop	68.33	224.68	60.53
Sharkskin	448.08	71.22	323.71

Table 2. Characterisation data for the microstructured surfaces.

3.3 Experimental apparatus

The experimental apparatus comprised of three main parts: the humidifier system, the condensation chamber, and data acquisition/control system (Figure 1b). The humidifier (LB7 by Steba) contained an ultrasonic water vaporiser, a temperature and %RH sensor and an air humidity control that delivered flows between 250 and 400 ml/hr [18]. The condensation chamber consisted of a 400 mm × 400 mm × 500 mm Perspex chamber with a visualisation window of 250 mm × 300 mm; a 100 mm diameter opening at the top for the entry of humid air from the humidifier; a 20 mm × 20 mm opening on the bottom side wall to connect the inserts with the data acquisition system and another similar opening at the bottom of the back wall to drain the condensate out of the chamber. The chamber was insulated with a 13 mm thick nitrile rubber sheet to reduce heat loss and surface condensation. There was an insulated testing support base of 180 mm × 130 mm inside the chamber for three inserts to be placed on, with a 20 mm separation between them. Each insert had a 0.9 m long bead wire subminiature type-K thermocouple probe (TP873 by Extech Instruments) attached near the microstructured surface. The inserts were completely insulated with waterproof insulating tape while leaving the top surface open for testing. The thermocouples were connected to a 3-Channel LCD temperature data logger (SD200 by Extech Instruments), with an accuracy

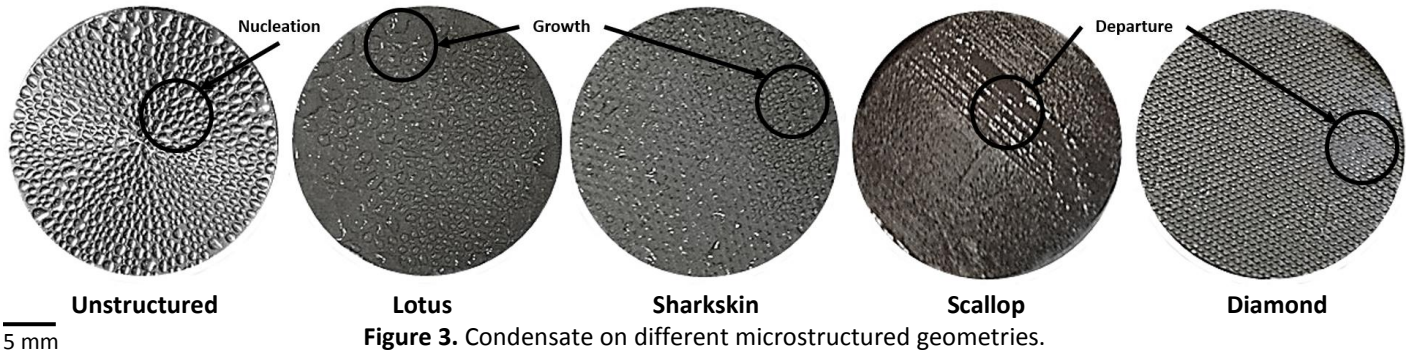

Figure 3. Condensate on different microstructured geometries.

of ±(0.5% + 0.5°C) from -100°C to +1300°C [19], which was part of the data acquisition/control system outside the chamber. The data acquisition/control system also consisted of a wireless temperature and humidity sensor with display (EkkoSensor ES-THD-02 by Ekkosense) inside the chamber with a temperature accuracy of ±0.5°C from 0°C to +40°C and a humidity accuracy of ±2% typical from 20% to 80% and ±5% maximum from 0% to 100% [20]. The displayed data was used to control the temperature inside the chamber using a fan that blew air through nichrome wire coils before starting the humidifier to increase the humidity in the chamber. A temperature, humidity and dew point data logger with an LCD screen was used to acquire and record the conditions inside the condensation chamber (EL-USB-2-LCD by EasyLog) with a temperature accuracy of ±0.55°C typically from 5°C to 60°C and a humidity accuracy of ±2.25% typically from 20% to 80% and ±3% maximum from 0% to 100% at temperatures up to 60°C [21].

4. RESULTS AND DISCUSSION

The differential temperature (ΔT) in the Diamond, Scallop, Sharkskin and Lotus surfaces was 26.32%, 21.05%, 15.79% and 7.89% higher than the unstructured surface, respectively. Thus, the highest ΔT was observed for the Diamond geometry (Table 3). Results can be supported by the experimental and numerical data obtained by Chatterjee et al. [10] with a 25% improvement, and Qi et al. [8] with 20% and 50% better heat transfer when using grooved surfaces.

	Unstructured	Lotus	Sharkskin	Scallop	Diamond
ΔT (K)	1.27	1.37	1.47	1.53	1.60
Errors	0.18	0.12	0.17	0.22	0.21

Table 3. Differential temperature (ΔT) results and standard errors of means.

Visualisation of the condensation after 8 mins, shown in Figure 3, displays an active DWC on the microstructured surfaces and an inversely proportional relationship between the droplet size and the ΔT, which is consistent with the studies conducted by Chatterjee et al. [10]. Furthermore, the three stages of a droplet life were observed during this study: nucleation, growth, and departure. The unstructured surface exhibited the first stage after 8 mins of condensation, while the Lotus and Sharkskin structured surfaces showed the second phase whereas the Diamond and Scallop surfaces were already in the final stage of a droplet life (Figure 3). Although droplets on the unstructured surface were evenly distributed, the droplet life cycle was longer on this insert compared to the other structured surfaces. From Figure 4, only three droplet life cycles are observed for the unstructured surface and the Lotus structure, while the Sharkskin and the Scallop structures exhibit five, and the Diamond structured surface displays six droplet life cycles. The droplet cycles of the individual structured surfaces are shown in Figure 5. According to Anand et al. [22], the removal of the condensate from the surface results in a significant increase in heat transfer. Grooten and Geld [23] also detailed that higher frequency of droplet removal reduces the probability of droplets sticking onto the condensation surface. These could in part explain the higher ΔT observed for the microstructured surfaces in the present study. While comparing among the various microstructures, the Diamond structure exhibited the highest ΔT (Table 3),

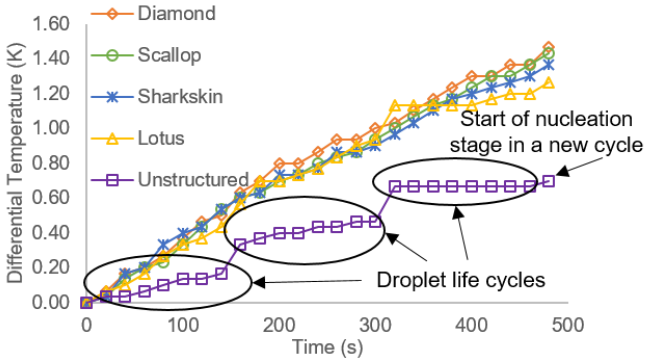

Figure 4. Differential Temperature (ΔT) vs. Time.

possibly due to the greater width and depth of the grooves with respect to the other structures (Table 2), thereby rendering a higher condensation rate as well as a greater drainage rate.

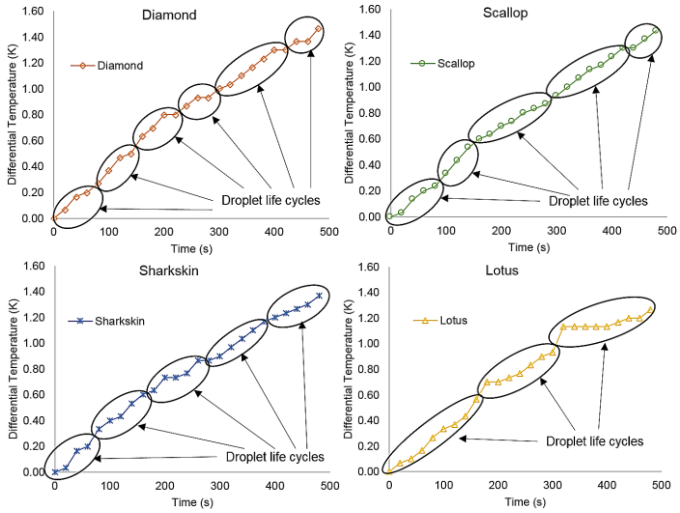

Figure 5. Droplet life cycles for the Diamond, Scallop, Sharkskin and Lotus structures.

5. CONCLUSIONS

Experimental data demonstrated that the differential temperatures were higher for all the microstructured surfaces with the Diamond structured insert exhibiting 1.26 times higher ΔT compared to the unstructured counterpart.

It is also concluded that the arrangement of the droplets and droplet life is considerably influenced by the design of the microstructure geometries. A comparison between the results from the current research and the previous experimental and numerical data exhibits similar trends which strongly supports the idea of using microstructured surfaces to enhance condensation heat transfer. Moreover, the results contribute to the basic understanding of condensation on microstructured surfaces and also suggest various geometries for an optimal droplet life that can ensure higher removal of the condensate. Nevertheless, it is imperative to undertake further research to ensure the successful reliability of heat transfer enhancement in humid environments for energy recovery purposes. Finally, this study opens up the possibility of using alternative manufacturing techniques such as laser microprocessing, micromilling, and nanomachining etc. for the creation of the microstructures, and analyse their effects on the prepared surfaces' performance during condensation.

ACKNOWLEDGEMENTS

The research was supported by The Mexican National Council on Science and Technology (CONACYT) and The Secretariat of Energy in Mexico (SENER) [Grant Number 327757/460766] as part of the PhD project 'High Peak, Perishable Energy Recovery - Foundation Phase'. Special acknowledgement is due to Mr Anuraag Saxena (CEng and MCIBSE) for his role in the construction of the experimental apparatus.

REFERENCE

[1] Renfer A, Tiwari MK, Tiwari R, Alfieri F, Brunschwiler T, Michel B, et al. Microvortex-enhanced heat transfer in 3D-integrated liquid cooling of electronic chip stacks. Int J Heat Mass Transf 2013;65:33–43. doi:10.1016/j.ijheatmasstransfer.2013.05.066.

[2] Orejon D, Shardt O, Gunda NSK, Ikuta T, Takahashi K, Takata Y, et al. Simultaneous dropwise and filmwise condensation on hydrophilic microstructured surfaces. Int J Heat Mass Transf 2017;114:187–97. doi:10.1016/j.ijheatmasstransfer.2017.06.023.

[3] Marschewski J, Brechbühler R, Jung S, Ruch P, Michel B, Poulikakos D. Significant heat transfer enhancement in microchannels with herringbone-inspired microstructures. Int J Heat Mass Transf 2016;95:755–64. doi:10.1016/j.ijheatmasstransfer.2015.12.039.

[4] Lorenzini-Gutierrez D, Hernandez-Guerrero A, Luviano-Ortiz JL, Leon-Conejo JC. Numerical and experimental analysis of heat transfer enhancement in a grooved channel with curved flow deflectors. Appl Therm Eng 2015;75:800–8. doi:10.1016/j.applthermaleng.2014.10.002.

[5] Kima SH, Lee GC, Kang JY, Moriyama K, HwanKim M, Park HS. Boiling heat transfer and critical heat flux evaluation of the pool boiling on micro structured surface. Int J Heat Mass Transf 2015;91:1140–7.

[6] Al-fahham M, Valera-Medina A, Marsh R. Experimental Study to Enhance Resistance for Boundary Layer Flashback in Swirl Burners Using Microsurfaces. ASME Turbo Expo 2017 2017:1–10.

[7] Kang Z, Wang L. Boiling heat transfer on surfaces with 3D-printing microstructures. Exp Therm Fluid Sci 2018;93:165–70. doi:10.1016/j.expthermflusci.2017.12.021.

[8] Qi B, Wei J, Li X. Enhancement of condensation heat transfer on grooved surfaces: Numerical analysis and experimental study. Appl Surf Sci 2017;115:1287–97.

[9] Atlantic Oceanographic and Meteorological Laboratory. How much energy does a hurricane release? 2014. http://www.aoml.noaa.gov/hrd/tcfaq/D7.html (accessed January 15, 2019).

[10] Chatterjee A, Derby MM, Peles Y, Jensen MK. Enhancement of condensation heat transfer with

patterned surfaces. Int J Heat Mass Transf 2014;71:675–81. doi:10.1016/j.ijheatmasstransfer.2013.12.069.
[11] Motoki S, Shimizu M, Kawahara G. Optimization of forced convection heat transfer by using a variational method. EFMC11, Seville, Spain: 2016.
[12] Cione JJ. The Relative Roles of the Ocean and Atmosphere as Revealed by Buoy Air–Sea Observations in Hurricanes. Mon Weather Rev 2014;143:904–13. doi:10.1175/mwr-d-13-00380.1.
[13] Al-fahham M, Bigot S, Valera-Medina A. A study of fluid flow characteristics using micro structured surfaces produced by WEDM. 4M / IWMF 2016;708.
[14] Jin Y, Herwig H. Turbulent flow and heat transfer in channels with shark skin surfaces: Entropy generation and its physical significance. Int J Heat Mass Transf 2014;70. doi:10.1016/j.ijheatmasstransfer.2013.10.063.
[15] Dean B, Bhushan B. Shark-skin surfaces for fluid-drag reduction in turbulent flow: a review. Philos Trans R Soc A Math Phys Eng Sci 2010;368:5737–5737. doi:10.1098/rsta.2010.0294.
[16] Bhushan B. Biomimetics: lessons from nature – an overview. Philos Trans R Soc A Math Phys Eng Sci 2009;367:1445–86. doi:10.1098/rsta.2009.0011.
[17] Al-fahham MAH. A Modelling and Experimental Study to Reduce Boundary Layer Flashback with Microstructure. Cardiff University, 2017. Ph.D. Thesis.
[18] Steba GB. LB 7 Humidifier 2019. https://stebagb.co.uk/product/lb-7-humidifier-130w/ (accessed May 8, 2019).
[19] Extech Instruments Corporation. 3-Channel Temperature Datalogger 2009. http://www.farnell.com/datasheets/1512711.pdf (accessed May 8, 2019).
[20] EkkoSense. EkkoSensor ES-THD-02 Wireless Temperature and Humidity sensor with Display 2019. https://www.ekkosense.com/wp-content/themes/ekkosense/media/EkkoSensor.pdf (accessed May 8, 2019).
[21] Lascar Electronics. EL-USB-2-LCD Temperature, Humidity and Dew Point Data Logger with LCD Screen 2016:1–5. http://www.farnell.com/datasheets/2581075.pdf (accessed May 8, 2019).
[22] Anand S, Rykaczewski K, Bengaluru Subramanyam S, Beysens D, Varanasi KK. How droplets nucleate and grow on liquids and liquid impregnated surfaces. Soft Matter 2015;11:69–80. doi:10.1039/c4sm01424c.
[23] Grooten MH, Geld CW. The importance of drainage in dropwise condensation from flowing air–steam mixtures. 14th Int. Heat Transf. Conf., 2010, p. 51–60.